Supplement of Atmos. Chem. Phys., 18, 10693–10713, 2018
https://doi.org/10.5194/acp-18-10693-2018-supplement

Supplement of

The secondary formation of organosulfates under interactions between biogenic emissions and anthropogenic pollutants in summer in Beijing

Yujue Wang et al.

Correspondence to: Min Hu (minhu@pku.edu.cn) and Jianzhen Yu (jian.yu@ust.hk)

Text S1 The influence of ion suppression on Orbitrap MS analysis

The overall molecular composition of S-containing organic species was measured using ESI-Orbitrap MS analysis. Sample matrix would influence the MS responses of different species, which cannot be eliminated (Furey et al., 2013). A previous study showed the extent of ion suppression was in good linearity with the concentrations/dilution factors of urine extracts (Chen et al., 2015). We conducted a set of experiments to evaluate the influence of sample matrix on MS response for OSs. A field blank sample, a clean sample and a polluted sample were extracted following the same procedures described in section 2.2. The sample collected during the nighttime of May 24 and 30 were selected to represent the clean sample and the polluted sample, respectively. Sample extracts were dried and re-dissolved either in acetonitrile/water (1:1) solvent or solvent containing 0.1 ppm α-pinene OS. The filter portion size and solvent volume were adjusted to yield solution containing ~100 μg or 200 μg OC/mL solvent for the clean sample and polluted sample. The OC concentrations are referred to as the OC loading before the SPE clean-up procedure. Only two concentration levels were examined due to the sample limitation. The intensity (signal-to-noise ratio, s/n) of α-pinene OS (0.1 ppm) in the three different sample matrixes were obtained by deducting the intensity of m/z=249.0802 in the same sample diluted by solvent without α-pinene OS (0.1 ppm) addition. The intensity in each sample was normalized by the ion injection time to make the intensities comparable (Kuang et al., 2016).

The intensity of 0.1 ppm α-pinene OS was the highest in the matrix of field blank extract and the lowest in the matrix of polluted sample extract. The extent of suppression ranged from 20% in the matrix of 100 μg OC from the clean sample to 62% in the matrix of 200 μg OC from the polluted sample (Fig. S1). It was clear that the extent of suppression increased with the OC content of the matrix, from 20% in 100 μg OC matrix to 32% in 200 μg OC matrix for the clean sample and from 45% in 100 μg OC matrix to 62% in 200 μg OC matrix for the polluted sample. The relative standard deviation (RSD) of α-pinene OS arising from different OC loadings (100 μg and 200 μg OC/mL solution) were 26% and 12% in polluted and clean samples, respectively. This result confirmed the benefit of adjusting OC content to a uniform level before Orbitrap MS analysis in minimizing the impact of matrix ion suppression. We note that when the sample was diluted to 100μg OC/mL solvent, the intensity of α-pinene OS in the clean sample was comparable to that in the field blank sample. This indicated that the ion suppression would be insignificant with less than 100 μg OC/mL solution. However, this level of dilution may limit the identification of species present at low concentrations due to too much dilution.

It is also apparent that chemical composition of the OC matrix also played a role in ion suppression. The RSD of α-pinene OS arising from different chemical composition (clean sample and polluted sample) were 40% and 27% in samples containing 200 μg and 100 μg OC/mL solution, respectively, which could represent the biggest differences of ion suppression arising from chemical composition. This source of difference in ion suppression could not be controlled with the infusion injection mode.

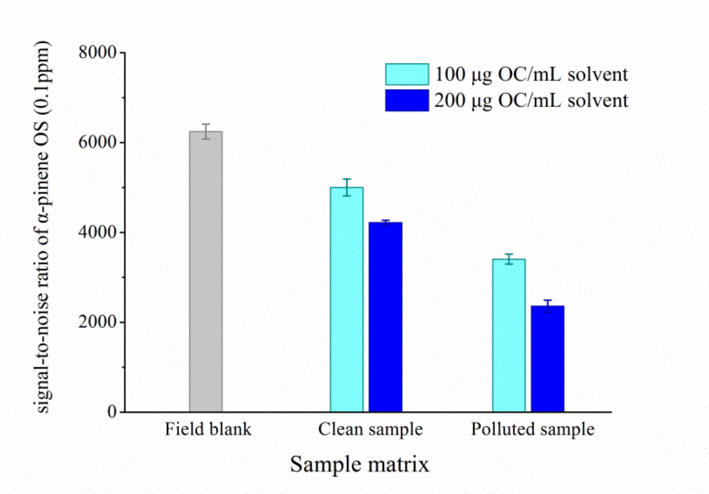

Figure S1 The intensity of α-pinene OS (0.1 ppm) in different sample matrix (blank sample, clean sample, polluted sample) with different OC loadings. The error bars were derived from three repeat injections of the same sample.

Text S2 The validation of ISORROPIA-II thermodynamic model prediction

The ISORROPIA-II thermodynamic model was run for metastable aerosols in this study. It has been suggested in previous studies that "metastable" state (only liquid phase) often showed better performance than the "stable" state (solid+ liquid) solution, and was commonly applied in previous pH or LWC predictions (Bougiatioti et al., 2016;Guo et al., 2015;Guo et al., 2016;Guo et al., 2017;Weber et al., 2016;Liu et al., 2017a). Though we lack direct evidence to reveal the physical state of ambient aerosols in this study, indirect evidence is provided to support that the assumption is reasonable. The verification of prediction by ISORROPIA-II was assessed by comparing the predicted and measured gaseous NH_3 in this study (Fig. S2) (Bougiatioti et al., 2016;Guo et al., 2015;Guo et al., 2016;Guo et al., 2017;Weber et al., 2016;Liu et al., 2017a). Good agreement was reached between predicted and measured gaseous ammonia concentrations (slope=0.99, intercept= 1.8 μg/m^3, R^2= 0.97). The result suggested that the "metastable" assumptions are reasonable in this study.

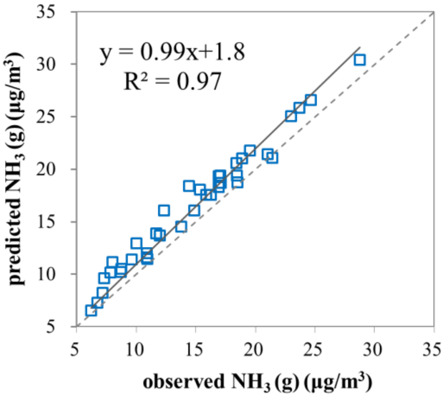

Figure S2 Comparison of predicted NH_3 (g) and measured NH_3 (g)

The ubiquitous existence of ambient metastable aerosols has been observed in previous studies (Rood et al., 1989). Based on our previous study in the winter of urban Beijing (Liu et al., 2017b), the rebound fraction of fine particles was ~0.8 at <20% RH, indicating a semisolid phase of particles. As the RH increased from 20 to 60%, the rebound fraction decreased from 0.8 to 0.2, suggesting transition from semisolid to liquid phase state. The rebound fraction of particles was lower than 0.4 at >40% RH, indicating that the liquid phase as the major phase state of ambient aerosols. RH conditions of < 20% were quite limited during the campaign. RH was usually higher than 40% and could increase to higher than 60% at night. Thus, a nearly liquid phase was likely the major phase state of ambient aerosols at night in this study. It would be desirable to obtain direct observational evidence of aerosol phase state in future studies.

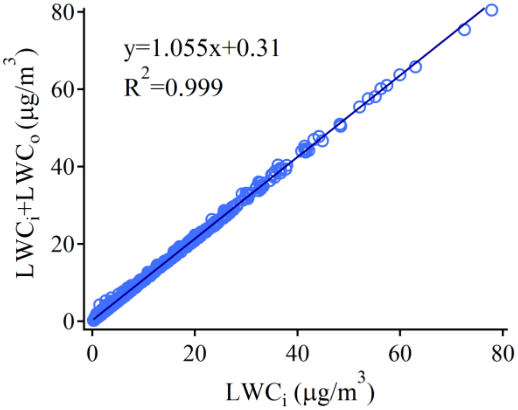

Figure S3 Comparison between aerosol liquid water content with or without water associated with organic compounds. LWC_i and LWC_o represent the water contributed by inorganic compounds and organic compounds, respectively. The data is from Fig. S1 in Wu et al. (2018) based on the measurement in Beijing (Wu et al., 2018).

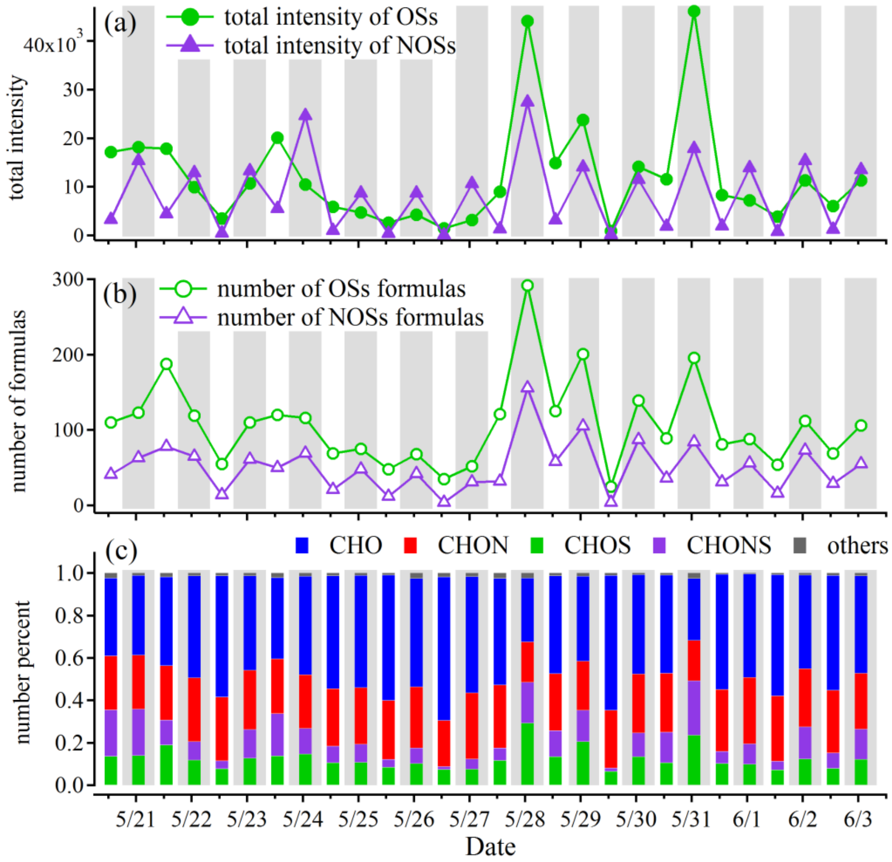

Figure S4 Temporal variation of the (a) total intensity and (b) total number of OSs and NOSs, and (c) temporal variation of the number percent of different compound categories. The gray background denotes the nighttime and white background denotes the daytime.

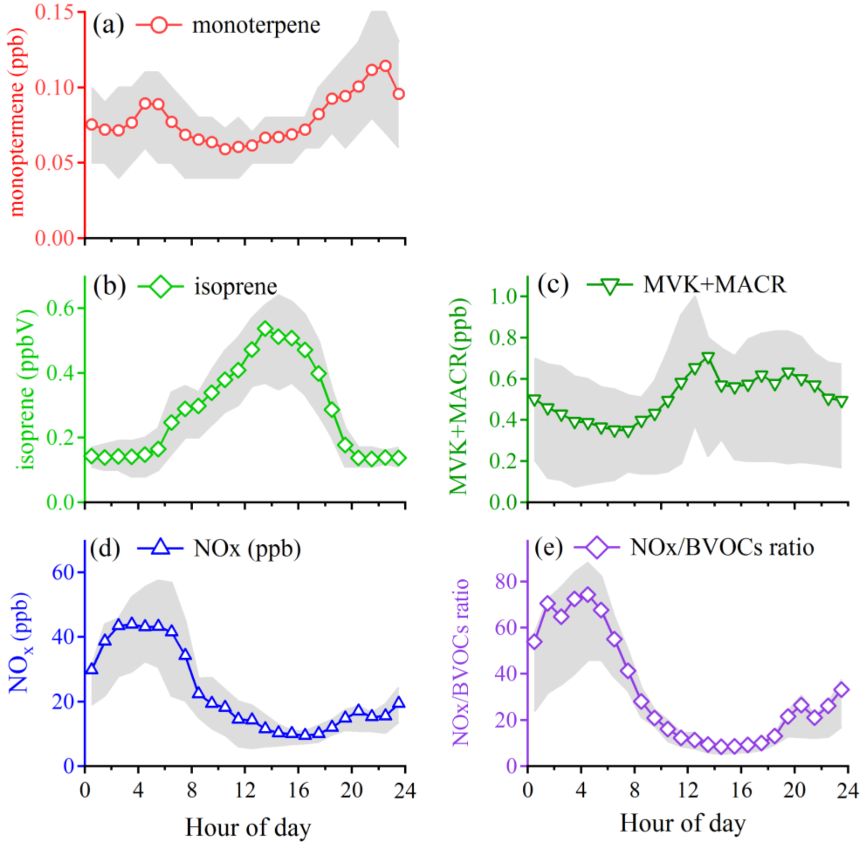

Figure S5 The diurnal variations of monoterpene, isoprene, NO_x and NO_x/BVOCs ratios

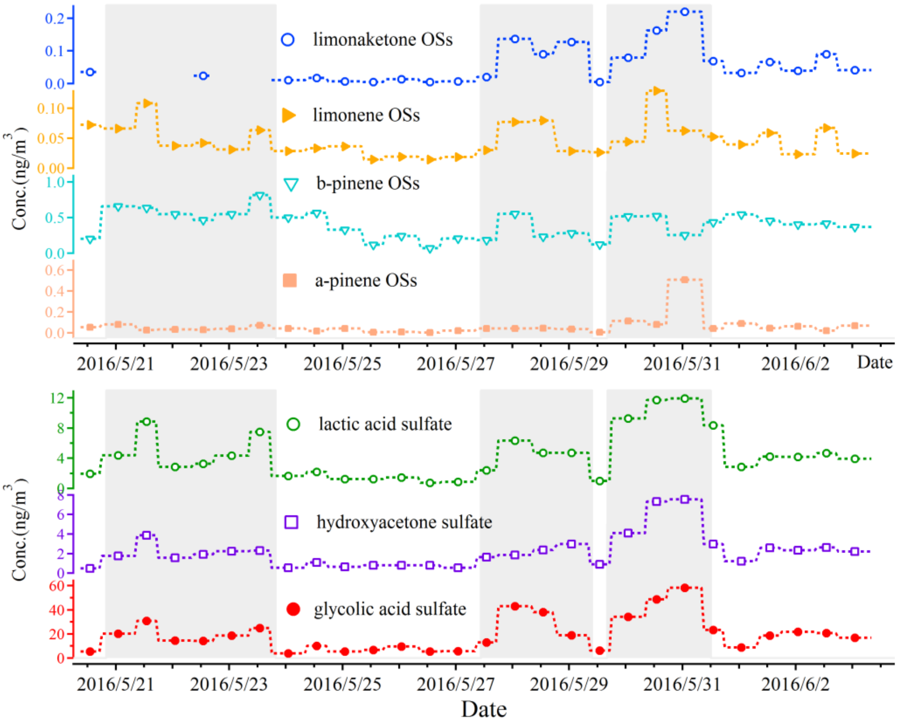

Figure S6 Time series of α-pinene OSs, β-pinene OSs, limonene OSs, limonaketone OSs, lactic acid sulfate, glycolic acid sulfate and hydroxyacetone sulfate. The pollution episodes were marked by gray shadow.

Table S1 The purity and recovery of organosulfate standards in this study

Organosulfate	Purity (%)	Recovery (%)
lactic acid sulfate	15%	
glycolic acid sulfate	8%	
α-pinene OS	>99%	80.5%
β-pinene OS	>99%	93.5%
limonene OS	>99%	85.4%
limonaketone OS	>99%	82.5%

Table S2 List of some most abundant OSs and NOSs peaks observed in the mass spectra

No.	**m/z [M-H]$^-$**	**Formula [M-H]$^-$**	**relative intensity (%)**			**precursor/ formation**	**references**
			05/24N	**05/30D**	**05/30N**		
organosulfates							
1	151.0071	$C_4H_7SO_4^-$	1	4.8	10.3	diesel fuel SOA	(Blair et al., 2017)
2	209.0489	$C_7H_{13}SO_5^-$	1	2.2	7.4	alkane	(Riva et al., 2016b)
3	223.0646	$C_8H_{15}SO_5^-$	3.1	9.7	16.8	diesel fuel SOA	(Blair et al., 2017)
4	225.0438	$C_7H_{13}SO_6^-$	0.4	2.3	14	diesel fuel SOA	(Blair et al., 2017)
5	235.0646	$C_9H_{15}SO_5^-$	12.9	8.7	9.1	diesel fuel SOA	(Blair et al., 2017)
6	237.0438	$C_8H_{13}SO_6^-$	1.4	3.3	10	diesel fuel SOA	(Blair et al., 2017)
7	237.0802	$C_9H_{17}SO_5^-$	2	5.4	9.4	alkane	(Riva et al., 2016b)
8	239.0595	$C_8H_{15}SO_6^-$		11.1	29.4	diesel fuel SOA	(Blair et al., 2017)
9	249.0802	$C_{10}H_{17}SO_5^-$	2.7	2.6	4.2	monoterpene	(Surratt et al., 2008;Wang et al., 2017)
10	251.0595	$C_9H_{15}SO_6^-$	3.7	9.5	24.7	monoterpene	(Wang et al., 2017)
11	251.0959	$C_{10}H_{19}SO_5^-$	1.9	5.3	7.5	alkane	(Riva et al., 2016b)
12	253.0751	$C_9H_{17}SO_6^-$	2	11.1	38	diesel fuel SOA	(Blair et al., 2017)
13	265.0751	$C_{10}H_{17}SO_6^-$	3	7.3	13.9	alkane	(Riva et al., 2016b)
14	267.0544	$C_9H_{15}SO_7^-$	2.1	19.4	100	alkane/ isoprene	(Riva et al., 2016a;Riva et al., 2016b)
15	267.0908	$C_{10}H_{19}SO_6^-$	1.6	6	13.4	diesel fuel SOA	(Blair et al., 2017)
16	269.0701	$C_9H_{17}SO_7^-$	0.3	4	15.8	alkane	(Riva et al., 2016b)
17	279.0544	$C_{10}H_{15}SO_7^-$	3.9	4.8	15.9	alkane	(Riva et al., 2016b)
18	279.0908	$C_{11}H_{19}SO_6^-$	1.9	5.5	13.3	diesel fuel SOA	(Blair et al., 2017)
19	279.1272	$C_{12}H_{23}SO_5^-$	2.2	3.3	6.5	alkane	(Riva et al., 2016b)
20	281.0701	$C_{10}H_{17}SO_7^-$	2.6	13.3	40	diesel fuel SOA	(Blair et al., 2017)
21	281.1064	$C_{11}H_{21}SO_6^-$	0.6	3.6	8.2	diesel fuel SOA	(Blair et al., 2017)
22	283.0493	$C_9H_{15}SO_8^-$	0.4	3.2	12.3	diesel fuel SOA	(Blair et al., 2017)
23	283.0857	$C_{10}H_{19}SO_7^-$	0.3	3.7	10.1	diesel fuel SOA	(Blair et al., 2017)
24	293.0701	$C_{11}H_{17}SO_7^-$	0.9		10.1	diesel fuel SOA	(Blair et al., 2017)

25	293.1064	$C_{12}H_{21}SO_6^-$	0.9		9.5		
26	295.0493	$C_{10}H_{15}SO_8^-$	1	2.5	7.1	alkane	(Riva et al., 2016b)
27	295.0857	$C_{11}H_{19}SO_7^-$	1.2	9	25.6	diesel fuel SOA	(Blair et al., 2017)
28	295.1221	$C_{12}H_{23}SO_6^-$	0.7	3.2	6.2	diesel fuel SOA	(Blair et al., 2017)
29	297.0650	$C_{10}H_{17}SO_8^-$		4.2	13.5	alkane	(Riva et al., 2016b)
30	307.0857	$C_{12}H_{19}SO_7^-$	0.6		9.7		
31	307.1221	$C_{13}H_{23}SO_6^-$			7.2		
32	307.1585	$C_{14}H_{27}SO_5^-$	2.1		7.6	diesel fuel SOA	(Blair et al., 2017)
33	309.1014	$C_{12}H_{21}SO_7^-$		11	25.7	diesel fuel SOA	(Blair et al., 2017)
34	321.1014	$C_{13}H_{21}SO_7^-$	0.5		7.5	diesel fuel SOA	(Blair et al., 2017)
35	321.1741	$C_{15}H_{29}SO_5^-$	1.6	6	7.7	diesel fuel SOA	(Blair et al., 2017)
36	325.0963	$C_{12}H_{21}SO_8^-$			10.2	diesel fuel SOA	(Blair et al., 2017)
37	339.0755	$C_{12}H_{19}SO_9^-$			8	diesel fuel SOA	(Blair et al., 2017)
38	351.1119	$C_{14}H_{23}SO_8^-$			9.4	diesel fuel SOA	(Blair et al., 2017)
39	365.1276	$C_{15}H_{25}SO_8^-$	0.3		7.6	diesel fuel SOA	(Blair et al., 2017)
40	373.0963	$C_{16}H_{21}SO_8^-$	5	9.5	8.7	diesel fuel SOA	(Blair et al., 2017)
nitrooxy-organosulfates							
1	276.0184	$C_9H_{10}NO_7S^-$	3.2		9.3		
2	284.0446	$C_8H_{14}NO_8S^-$	6.9	3	10.4		
3	294.0653	$C_{10}H_{16}NO_7S^-$	67.3	5	82.9	monoterpene	(Surratt et al., 2008)
4	296.0446	$C_9H_{14}NO_8S^-$	23.2	1.4	9	monoterpene	(Surratt et al., 2008)
5	300.0395	$C_8H_{14}NO_9S^-$	3.9	2.5	19.2		
6	312.0759	$C_{10}H_{18}NO_8S^-$	10.1		11.5		
7	314.0551	$C_9H_{16}NO_9S^-$	1.9		14.6		
8	326.0551	$C_{10}H_{16}NO_9S^-$	23.9	4	29.2	monoterpene	(Surratt et al., 2008)
9	328.0708	$C_{10}H_{18}NO_9S^-$	3.3	2.5	9.4	monoterpene	(Surratt et al., 2008)
10	342.0500	$C_{10}H_{16}NO_{10}S^-$	8.3	3.3	23.3	monoterpene	(Surratt et al., 2008)

Table S3 Summery of OSs and NOSs concentrations (ng/m^3) in previous studies and this study

Location	**date**	**Total OSs**	**HAS**	**GAS**	**LAS**	**Isoprene OSs**			**Isoprene NOSs**	**Monoterpene OSs**				**Monoterpene NOSs**		**references**
						$C_4H_7O_7S^-$	$C_5H_7O_7S^-$	$C_5H_{11}O_7S^-$	$C_5H_{10}NO_9S^-$	α-pinene OSs	β-pinene OSs	Limonene OSs	Limonaketone OSs	$C_{10}H_{16}NO_7S^-$	$C_9H_{14}NO_8S^-$	
Riverside, California, US	July, 2005	4.1		3.3	0.8											(Olson et al., 2011)
Cleveland, Ohio, US	July, 2007	2.3		1.9	0.4											(Olson et al., 2011)
Bakersfield, California, US	June, 2010	5.2-6.0		4.5- 5.4	0.6-0.7											(Olson et al., 2011)
Centreville, Alabama, US	June- July, 2013	20.3-42.9	2.7-5.8	8- 20.6	9.6-19											(Hettiyadura et al., 2015;Hettiyadura et al., 2017)
Birmingham, Alabama, US	June- July, 2013	202.5	0.2	26.2	2.7	7.2	1.4	164.5	0.3							(Rattanavaraha et al., 2016)
Tennessee, US	June- July, 2013	179.5				10		169.5								(Budisulistiorini et al., 2015)
Towson, mid-Atlantic, US	August 2012- June 2013	8.4-33.0	0.3-0.8		0.8-1.3	0.2-4.4		1.6-18.3				0.1-0.4		0.1-2	0.1-0.3	(Meade et al., 2016)
Mexico city, Mexico	March, 2006	5.3-8.8		4.1- 7.0	1.2-1.8											(Olson et al., 2011)
Bavaria, Germany	July, 2002	23.4									23.4					(Iinuma et al., 2009)
Brasschaat, Belgium	June- July, 2007		0.12-36.7					2.0-9.0	0.14-2.3					0.63-3.6		(Gómez-González et al., 2012)
Lahore, Pakistan	Nov., 2007	15.1		11.3	3.8											(Olson et al., 2011)
Pearl River Delta (PRD), China	Sep. 2010	53					0.68							52		(He et al., 2014)
	Nov. 2010	151					0.38							151		
Guangdong, China	Nov.-Dec., 2010	2.71								0.41	0.19	1.14	0.97			(Wang et al., 2017)
Hong Kong, China	Nov.-Dec., 2010	0.88								0.08	0.06	0.36	0.38			
Beijing, China	May-June, 2016	55.2	2.2	19.5	4.4	3.6	5.9	5.3	1.4	0.06	0.4	0.05	0.06	12.0	0.4	this study

Table S4 The pearson correlations between individual OSs and NOSs species quantified by HPLC-MS as well as their correlations with aerosol components, acidity, LWC, VOC precursors and oxidants (n=28)

	total OSs	HAS	GAS	LAS	isoprene OSs			isoprene NOS	α-pinene OSs	β-pinene OSs	Limonene OSs	Limonaketone OSs	monoterpene NOSs	
		$C_3H_5O_5S^-$	$C_2H_3O_6S^-$	$C_3H_5O_6S^-$	$C_4H_7O_7S^-$	$C_5H_7O_7S^-$	$C_5H_{11}O_7S^-$	$C_5H_{10}NO_9S^-$	$C_{10}H_{17}O_5S^-$	$C_{10}H_{17}O_5S^-$	$C_{10}H_{17}O_5S^-$	$C_9H_{15}O_6S^-$	$C_{10}H_{16}NO_7S^-$	$C_9H_{14}NO_8S^-$
total OSs	1.00													
$C_3H_5O_5S^-$	**0.96**	1.00												
$C_2H_3O_6S^-$	**0.97**	**0.88**	1.00											
$C_3H_5O_6S^-$	**0.93**	**0.92**	**0.91**	1.00										
$C_4H_7O_7S^-$	**0.95**	**0.97**	**0.86**	**0.86**	1.00									
$C_5H_7O_7S^-$	**0.99**	**0.96**	**0.95**	**0.93**	**0.95**	1.00								
$C_5H_{11}O_7S^-$	**0.84**	**0.91**	**0.73**	**0.72**	**0.93**	**0.85**	1.00							
$C_5H_{10}NO_9S^-$	**0.86**	**0.82**	**0.83**	**0.79**	**0.83**	**0.88**	**0.76**	1.00						
$C_{10}H_{17}O_5S^-$	**0.67**	0.68	0.63	0.59	0.67	0.67	**0.71**	**0.84**	1.00					
$C_{10}H_{17}O_5S^-$	0.18	0.22	0.29	0.44	0.20	0.31	(0.03)	0.26	0.01	1.00				
$C_{10}H_{17}O_5S^-$	**0.64**	0.62	0.69	0.71	0.56	0.67	0.37	0.39	0.20	0.44	1.00			
$C_9H_{15}O_6S^-$	**0.82**	**0.84**	**0.76**	**0.73**	**0.82**	**0.79**	**0.86**	**0.74**	**0.76**	(0.04)	0.48	1.00		
$C_{10}H_{16}NO_7S^-$	0.15	0.11	0.26	0.18	0.13	0.25	0.10	0.48	0.40	0.29	(0.14)	0.10	1.00	
$C_9H_{14}NO_8S^-$	(0.02)	0.02	0.07	0.02	0.02	0.10	0.06	0.26	0.32	0.19	(0.18)	0.07	**0.79**	1.00
SO_4^{2-}	**0.67**	**0.58**	**0.69**	**0.64**	**0.59**	**0.69**	0.42	**0.67**	**0.57**	0.16	**0.67**	0.44	0.19	(0.03)
NH_4^+	0.54	0.42	0.59	0.55	0.43	0.57	0.22	0.58	0.44	0.26	0.62	0.24	0.18	(0.07)
NO_3^-	0.22	0.09	0.31	0.32	0.06	0.23	(0.11)	0.36	0.21	0.48	0.39	0.00	0.21	(0.09)
LWC	**0.55**	0.40	**0.61**	**0.54**	0.39	**0.57**	0.23	**0.68**	**0.57**	0.37	0.47	0.29	0.43	0.18
Organics	**0.64**	**0.55**	**0.65**	**0.64**	**0.57**	**0.65**	0.45	**0.58**	0.42	0.43	**0.56**	0.48	0.38	0.05
Liquid [H^+]	**0.67**	**0.64**	**0.65**	**0.57**	**0.67**	**0.68**	**0.60**	**0.61**	**0.58**	(0.14)	**0.57**	**0.52**	0.09	(0.00)

isoprene	0.32	0.34	0.29	0.30	0.34	0.31	0.28	0.03	(0.07)	(0.03)	0.64	0.37	(0.64)	(0.70)
MVK+MACR	0.73	**0.72**	**0.69**	**0.67**	**0.71**	**0.75**	**0.63**	**0.69**	0.53	0.06	0.64	0.71	0.05	(0.22)
monoterpene	0.35	0.29	0.38	0.36	0.27	0.40	0.11	0.44	0.19	0.34	0.28	0.22	0.55	0.23
NO_2	0.35	0.27	0.37	0.32	0.29	0.37	0.18	**0.58**	0.41	0.30	0.01	0.20	**0.76**	0.39
O_3	0.45	0.47	0.40	0.39	0.51	0.45	0.44	0.20	0.16	(0.14)	0.67	0.43	(0.59)	(0.57)
O_x (NO_2+O_3)	0.57	0.58	0.53	0.50	0.62	0.59	0.51	0.39	0.29	(0.05)	0.71	0.51	(0.39)	(0.48)

Table S5 The back trajectories, VOC precursors, and oxidants during the three episodes

Episode	Isoprene (ppb)	MVK+MACR (ppb)	Monoterpene (ppb)	NO_2 (ppb)	O_3 (ppb)	O_x (NO_2+O_3) (ppb)	Back trajectories
episode I (23 May day)	0.36	0.50	0.06	22.51	55.47	77.98	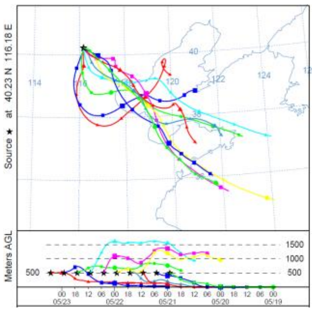
episode II (27 May night)	0.22	0.43	0.13	24.83	38.27	63.10	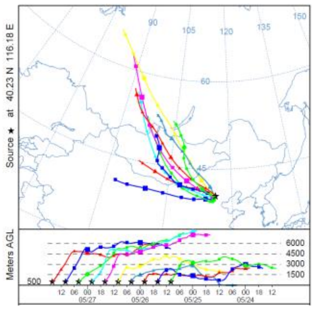
episode III (30 May night)	0.23	1.00	0.08	29.77	87.56	117.33	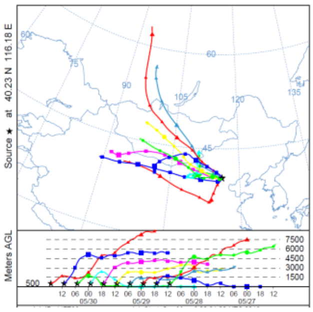

References

Blair, S. L., MacMillan, A. C., Drozd, G. T., Goldstein, A. H., Chu, R. K., Pasa-Tolic, L., Shaw, J. B., Tolic, N., Lin, P., Laskin, J., Laskin, A., and Nizkorodov, S. A.: Molecular Characterization of Organosulfur Compounds in Biodiesel and Diesel Fuel Secondary Organic Aerosol, Environ. Sci. Technol., 51, 119-127, 10.1021/acs.est.6b03304, 2017.

Bougiatioti, A., Nikolaou, P., Stavroulas, I., Kouvarakis, G., Weber, R., Nenes, A., Kanakidou, M., and Mihalopoulos, N.: Particle water and pH in the eastern Mediterranean: source variability and implications for nutrient availability, Atmos. Chem. Phys., 16, 4579-4591, 10.5194/acp-16-4579-2016, 2016.

Budisulistiorini, S. H., Li, X., Bairai, S. T., Renfro, J., Liu, Y., Liu, Y. J., McKinney, K. A., Martin, S. T., McNeill, V. F., Pye, H. O. T., Nenes, A., Neff, M. E., Stone, E. A., Mueller, S., Knote, C., Shaw, S. L., Zhang, Z., Gold, A., and Surratt, J. D.: Examining the effects of anthropogenic emissions on isoprene-derived secondary organic aerosol formation during the 2013 Southern Oxidant and Aerosol Study (SOAS) at the Look Rock, Tennessee ground site, Atmos. Chem. Phys., 15, 8871-8888, 10.5194/acp-15-8871-2015, 2015.

Chen, G. Y., Liao, H. W., Tseng, Y. J., Tsai, I. L., and Kuo, C. H.: A matrix-induced ion suppression method to normalize concentration in urinary metabolomics studies using flow injection analysis electrospray ionization mass spectrometry, Anal. Chim. Acta, 864, 21-29, 10.1016/j.aca.2015.01.022, 2015.

Furey, A., Moriarty, M., Bane, V., Kinsella, B., and Lehane, M.: Ion suppression; a critical review on causes, evaluation, prevention and applications, Talanta, 115, 104-122, 10.1016/j.talanta.2013.03.048, 2013.

Gómez-González, Y., Wang, W., Vermeylen, R., Chi, X., Neirynck, J., Janssens, I. A., Maenhaut, W., and Claeys, M.: Chemical characterisation of atmospheric aerosols during a 2007 summer field campaign at Brasschaat, Belgium: sources and source processes of biogenic secondary organic aerosol, Atmos. Chem. Phys., 12, 125-138, 10.5194/acp-12-125-2012, 2012.

Guo, H., Xu, L., Bougiatioti, A., Cerully, K. M., Capps, S. L., Hite, J. R., Carlton, A. G., Lee, S. H., Bergin, M. H., Ng, N. L., Nenes, A., and Weber, R. J.: Fine-particle water and pH in the southeastern United States, Atmos. Chem. Phys., 15, 5211-5228, 10.5194/acp-15-5211-2015, 2015.

Guo, H., Sullivan, A. P., Campuzano-Jost, P., Schroder, J. C., Lopez-Hilfiker, F. D., Dibb, J. E., Jimenez, J. L., Thornton, J. A., Brown, S. S., Nenes, A., and Weber, R. J.: Particle pH and the Partitioning of Nitric Acid during Winter in the Northeastern United States, J. Geophys. Res., [Atmos.], 121, 10355-10376, 10.1002/2016JD025311, 2016.

Guo, H., Weber, R. J., and Nenes, A.: High levels of ammonia do not raise fine particle pH sufficiently to yield nitrogen oxide-dominated sulfate production, Scientific reports, 7, 12109, 10.1038/s41598-017-11704-0, 2017.

He, Q. F., Ding, X., Wang, X. M., Yu, J. Z., Fu, X. X., Liu, T. Y., Zhang, Z., Xue, J., Chen, D. H., Zhong, L. J., and Donahue, N. M.: Organosulfates from pinene and isoprene over the Pearl River Delta, South China: seasonal variation and implication in formation mechanisms, Environ. Sci. Technol., 48, 9236-9245, 10.1021/es501299v, 2014.

Hettiyadura, A. P. S., Stone, E. A., Kundu, S., Baker, Z., Geddes, E., Richards, K., and Humphry, T.: Determination of atmospheric organosulfates using HILIC chromatography with MS detection, Atmos. Meas. Tech., 8, 2347-2358, 10.5194/amt-8-2347-2015, 2015.

Hettiyadura, A. P. S., Jayarathne, T., Baumann, K., Goldstein, A. H., de Gouw, J. A., Koss, A., Keutsch, F. N., Skog, K., and Stone, E. A.: Qualitative and quantitative analysis of atmospheric organosulfates in Centreville, Alabama, Atmos. Chem. Phys., 17, 1343-1359, 10.5194/acp-17-1343-2017, 2017.

Iinuma, Y., Boge, O., Kahnt, A., and Herrmann, H.: Laboratory chamber studies on the formation of organosulfates from reactive uptake of monoterpene oxides, Phys. Chem. Chem. Phys., 11, 7985-7997, 10.1039/b904025k, 2009.

Kuang, B. Y., Lin, P., Hu, M., and Yu, J. Z.: Aerosol size distribution characteristics of organosulfates in the Pearl River Delta region, China, Atmos. Environ., 130, 23-35, 10.1016/j.atmosenv.2015.09.024, 2016.

Liu, M., Song, Y., Zhou, T., Xu, Z., Yan, C., Zheng, M., Wu, Z., Hu, M., Wu, Y., and Zhu, T.: Fine particle pH during severe haze episodes in northern China, Geophys. Res. Lett., 44, 5213-5221, 10.1002/2017gl073210, 2017a.

Liu, Y., Wu, Z., Wang, Y., Xiao, Y., Gu, F., Zheng, J., Tan, T., Shang, D., Wu, Y., Zeng, L., Hu, M., Bateman, A. P., and Martin, S. T.: Submicrometer Particles Are in the Liquid State during Heavy Haze Episodes in the Urban Atmosphere of Beijing, China, Environmental Science & Technology Letters, 4, 427-432, 10.1021/acs.estlett.7b00352, 2017b.

Meade, L. E., Riva, M., Blomberg, M. Z., Brock, A. K., Qualters, E. M., Siejack, R. A., Ramakrishnan, K., Surratt, J. D., and Kautzman, K. E.: Seasonal variations of fine particulate organosulfates derived from biogenic and anthropogenic hydrocarbons in the mid-Atlantic United States, Atmos. Environ., 145, 405-414, 10.1016/j.atmosenv.2016.09.028, 2016.

Olson, C. N., Galloway, M. M., Yu, G., Hedman, C. J., Lockett, M. R., Yoon, T., Stone, E. A., Smith, L. M., and Keutsch, F. N.: Hydroxycarboxylic acid-derived organosulfates: synthesis, stability, and quantification in ambient aerosol, Environ. Sci. Technol., 45, 6468-6474, 10.1021/es201039p, 2011.

Rattanavaraha, W., Chu, K., Budisulistiorini, S. H., Riva, M., Lin, Y.-H., Edgerton, E. S., Baumann, K., Shaw, S. L., Guo, H., King, L., Weber, R. J., Neff, M. E., Stone, E. A., Offenberg, J. H., Zhang, Z., Gold, A., and Surratt, J. D.: Assessing the impact of anthropogenic pollution on isoprene-derived secondary organic aerosol formation in $PM_{2.5}$ collected from the Birmingham, Alabama, ground site during the 2013 Southern Oxidant and Aerosol Study, Atmos. Chem. Phys., 16, 4897-4914, 10.5194/acp-16-4897-2016, 2016.

Riva, M., Budisulistiorini, S. H., Zhang, Z., Gold, A., and Surratt, J. D.: Chemical characterization of secondary organic aerosol constituents from isoprene ozonolysis in the presence of acidic aerosol, Atmos. Environ., 130, 5-13, 10.1016/j.atmosenv.2015.06.027, 2016a.

Riva, M., Da Silva Barbosa, T., Lin, Y.-H., Stone, E. A., Gold, A., and Surratt, J. D.: Chemical characterization of organosulfates in secondary organic aerosol derived from the photooxidation of alkanes, Atmos. Chem. Phys., 16, 11001-11018, 10.5194/acp-16-11001-2016, 2016b.

Rood, M. J., Shaw, M. A., Larson, T. V., and Covert, D. S.: Ubiquitous nature of ambient metastable aerosol, Nature, 337, 537-539, 10.1038/337537a0, 1989.

Surratt, J. D., Gomez-Gonzalez, Y., Chan, A. W., Vermeylen, R., Shahgholi, M., Kleindienst, T. E., Edney, E. O., Offenberg, J. H., Lewandowski, M., Jaoui, M., Maenhaut, W., Claeys, M., Flagan, R. C., and Seinfeld, J. H.: Organosulfate formation in biogenic secondary organic aerosol, J. Phys. Chem. A, 112, 8345-8378, 10.1021/jp802310p, 2008.

Wang, Y., Ren, J., Huang, X. H. H., Tong, R., and Yu, J. Z.: Synthesis of Four Monoterpene-Derived Organosulfates and Their Quantification in Atmospheric Aerosol Samples, Environ. Sci. Technol., 51, 6791-6801, 10.1021/acs.est.7b01179, 2017.

Weber, R. J., Guo, H., Russell, A. G., and Nenes, A.: High aerosol acidity despite declining atmospheric sulfate concentrations over the past 15 years, Nature Geosci., 9, 282-285, 10.1038/ngeo2665, 2016.

Wu, Z. J., Wang, Y., Tan, T. Y., Zhu, Y. S., Li, M. R., Shang, D. J., Wang, H. C., Lu, K. D., Guo, S., Zeng, L. M., and Zhang, Y. H.: Aerosol Liquid Water Driven by Anthropogenic Inorganic Salts: Implying Its Key Role in Haze Formation over the North China Plain, Environmental Science & Technology Letters, 5, 160-166, 10.1021/acs.estlett.8b00021, 2018.